PHYSICAL REVIEW C **68**, 031301(R) (2003)

Prolate-oblate phase transition in the Hf-Hg mass region

J. Jolie and A. Linnemann
Institute of Nuclear Physics, University of Cologne, Zülpicherstrasse 77, 50937 Cologne, Germany
(Received 22 October 2002; revised manuscript received 12 March 2003; published 17 September 2003)

Experimental data in the Hf-Hg mass region indicate the presence of a prolate-oblate phase transition. The transition in which γ-soft nuclei exhibit a first-order quantum phase transition in their shape is of the type that was recently proposed on very general grounds using Landau theory. The transition is situated close to the O(6) limit of the interacting boson model which is indeed found empirically in this mass region. Our study also hints at explaining why the quadrupole moments in Pt isotopes deviate from the O(6) value and confirms the recently proposed prolate-oblate phase transition with experimental data.

DOI: 10.1103/PhysRevC.68.031301 PACS number(s): 21.60.Fw, 21.10.Gv, 21.10.Ky, 27.80.+w

Recently, the topic of quantum phase transitional behavior of atomic nuclei has received a lot of attention, when it was shown that new symmetries, called X(5) and E(5), can describe atomic nuclei at the critical points [1,2] within the framework of the collective model [3]. The phase transitions considered in these references are those of the ground state deformation, which can conveniently be described by the deformation parameters β and γ defining the form of the nuclear ellipsoid [3]. Remarkably, the parameter free predictions provided by these symmetries are closely realized in some atomic nuclei [4,5].

Following these observations we have shown that γ-soft nuclei, which are also analytically solvable, are located exactly at a previously unrecognized phase transition [6]. Here the symmetry at the critical point is the well known O(6) dynamical symmetry of the interacting boson model (IBM) [7], which describes atomic nuclei as an interacting system of s and d bosons made up of the valence nucleons. The prolate-oblate first-order phase transition occurs when one crosses a path extending from O(6) towards the U(5) limit up to the point where the atomic nucleus becomes spherical. At this point the transition is of second order. The new first-order phase transition completes the equilibrium nuclear phase diagram and allows a general interpretation of all observed shape phase transitions of the IBM within the Landau theory of phase transitions [8]. Note that strictly speaking the phase transitions occur only when the number of bosons $N \rightarrow \infty$.

The resulting shape phase diagram is shown in Fig. 1. It is parametrized using the simple Hamiltonian

$$\hat{H}(N,\eta,\chi) = \eta\,\hat{n}_d + \frac{\eta-1}{N}\hat{Q}_\chi \cdot \hat{Q}_\chi, \qquad (1)$$

where $\hat{n}_d = d^\dagger \cdot \tilde{d}$ is the d-boson number operator and $\hat{Q}_\chi = (s^\dagger \tilde{d} + d^\dagger s)^{(2)} + \chi (d^\dagger \times \tilde{d})^{(2)}$ is the quadrupole operator. N in the denominator stands for the total number of bosons. The parameters η and χ vary within the range $\eta \in [0,1]$ and $\chi \in [-\sqrt{7}/2, +\sqrt{7}/2]$.

While the Hamiltonian is extremely simple, the structures it generates with its two parameters η and χ are very rich [8,9]. Within the restricted parameter range, describing the extended Casten triangle, there are four dynamical symmetries of the IBM, three first-order phase transitions and one isolated second-order phase transition (see Fig. 1). Out of the four dynamical symmetries three, called U(5), SU(3), and $\overline{\mathrm{SU(3)}}$ limits, are located in the vertices. They correspond to vibrational nuclei with a spherical form [U(5)], an axially symmetric prolate rotor with a minimum in the energy at $\gamma = 0°$ [SU(3)], and an axially symmetric oblate rotor with a minimum at $\gamma = 60°$ [$\overline{\mathrm{SU(3)}}$]. The fourth symmetry is located in the middle of the SU(3)-$\overline{\mathrm{SU(3)}}$ leg and corresponds to a rotor with a flat potential in γ [O(6)]. Note that, here, we use the convention of Dieperink, Scholten, and Iachello [10] with $\beta \geqslant 0$ and $0° \leqslant \gamma \leqslant 60°$.

It is the purpose of this work to present a reinterpretation of atomic nuclei in the Hf-Hg mass region in the context of the prolate-oblate phase transition passing through the O(6) limit [6]. These nuclei are known to be situated close to the upper right leg of the triangle in Fig. 1 with $\eta = 0$ [11,12]. Although oblate nuclei or transitions from γ soft to oblate shapes are rare they do occur in the heavy platinum and mercury isotopes close to ^{196}Pt. In order to avoid confusion we would like to stress that here we are dealing with the normal hole configurations and not with the oblate multiparticle-multihole excitations that are observed in addition to the normal states in the light Pt, Hg, and Pb isotopes [13].

In Fig. 2 we show typical observables that can be used to locate an atomic nucleus in the shape phase diagram. They are the ratio $R_{4/2}$ of the excitation energies of the first 4^+ and 2^+ states, the spectroscopic quadrupole moment $Q(2_1^+)$ of the first 2^+ state and the $B(E2; 2_2^+ \rightarrow 2_1^+)$ value. These quantities are calculated for the realistic value of $N = 10$. For the electromagnetic observables the electric quadrupole transition operator,

$$T(E2) = e[(s^\dagger \tilde{d} + d^\dagger s)^{(2)} + \chi (d^\dagger \tilde{d})^{(2)}], \qquad (2)$$

was used in the consistent-Q formalism [12], i.e., with the same χ value as the Hamiltonian. As this choice yields nonzero quadrupole moments for nuclei in the spherical phase when $\chi \neq 0$, we have plotted the signatures on a square rather than on the extended triangle. One clearly notices in Fig. 2 that the variations are the sharpest around $\chi = 0$ on the SU(3)-$\overline{\mathrm{SU(3)}}$ side. The signatures are chosen because each

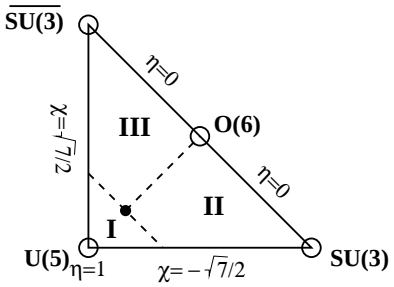

FIG. 1. The extended Casten triangle [6] and its different phases: spherical nuclei (phase I) and deformed nuclei with prolate (phase II), and oblate (phase III) shape. The open circles indicate the location of the IBM dynamical symmetries. The solid dot in the center represent the triple point of nuclear deformation [8], where all phases coalesce. The dashed lines correspond to the first-order shape phase transitions.

reveals important structural information. A small $Q(2_1^+)$ and large $B(E2;2_2^+ \rightarrow 2_1^+)$ situate a nucleus along the U(5)-O(6) line. Along this line $R_{4/2}$ varies from near 2.0 at U(5) to near 2.5 at O(6). Going towards SU(3) and $\overline{\text{SU(3)}}$ the $R_{4/2}$ ratio increases rapidly to 3.33 and the experimental quadrupole moment attains large negative values towards prolate SU(3) and positive towards oblate $\overline{\text{SU(3)}}$. In the same direction there is a steep decrease of the $B(E2;2_2^+ \rightarrow 2_1^+)$ value which is strictly forbidden for SU(3)- and $\overline{\text{SU(3)}}$-like nuclei. The same transition is collective, albeit varying, on the U(5)-O(6) line.

To summarize, in a $\text{SU(3)}-\text{O(6)}-\overline{\text{SU(3)}}$ transitional region, $R_{4/2}$ ratios around and above 2.5 need to be observed. The experimental quadrupole moment, which is related to the order parameter [8], should change sign and increase rapidly when going away from location of the prolate-oblate transition, whereby $Q(2_1^+)$ is negative for SU(3)-like, positive for $\overline{\text{SU(3)}}$-like, and zero for the γ-unstable O(6)-like nuclei. The $B(E2;2_2^+ \rightarrow 2_1^+)$ value should peak with a collective value at O(6) and then decrease quickly as $|\chi|$ increases.

While the quadrupole moment provides a clear signature for the deformation, it is more difficult to clearly distinguish where a given nucleus is situated between the O(6) and U(5) limits, although the $R_{4/2}$ gives an indication. This is due to the fact that the Hamiltonian in Eq. (1) conserves the O(5) symmetry when $\chi=0$. We first examine the situation for the Pt isotopes in more detail. Atomic nuclei representing the O(6) structure are classified by $|N,\sigma,\tau,L\rangle$ with the labels N,σ,τ, and L given by the irreps of the U(6), O(6), O(5), and O(3) groups. From structural point of view the lowest states are formed by those states with the maximal value $\sigma=N$. The next class of states have $\sigma=N-2, N-4, \ldots,$ 1 or 0. Within a given σ the τ values can take the values $\tau=0,1,2,\ldots,\sigma$. The wave functions consist of either odd (even) numbers of d bosons when τ is odd (even). Therefore the quadrupole moments vanish since $\chi=0$. Besides this property selection rules allow $|\Delta\tau|=1$ transitions, yielding the nonzero $B(E2;2_2^+ \rightarrow 2_1^+)$ transition rates, and forbid the $|\Delta\tau|=0$ and $|\Delta\sigma|\neq 0$ transitions. The latter selection rule allows the most direct distinction between O(6)- and U(5)-like nuclei. It involves, however, the knowledge of absolute $B(E2)$ values of highly excited low-spin states which are only known in a few nuclei. The atomic nucleus ^{196}Pt was proposed in Ref. [14] as an excellent example of the O(6) limit of the IBM. While this was strongly debated, due to the nonvanishing quadrupole moment of $Q(2_1^+) = +0.66(12)e$ b [15], the O(6) character was clearly established for ^{196}Pt [16,17] by the $|\Delta\sigma|$ selection rule, which allows to place this nucleus near $\eta=0$.

In an attempt to span a larger part of the extended Casten triangle we investigate the mass region around ^{196}Pt, going down to ^{180}Hf where the nuclear shape is already well described by a prolate ellipsoid. To have a smooth variation in structure a series of isotopes with varying boson number N, $N=N_\pi+N_\nu$, was chosen which fulfilled the following two conditions: the sequence involved atomic nuclei which differ from each other by one boson number and the three signatures needed to be experimentally known. The sequence obtained was ^{180}Hf, ^{182,184,186}W, ^{188,190,192}Os, ^{194,196}Pt, and ^{198,200}Hg which spans in a uniform way boson numbers from $N=14$ down to $N=4$.

In order to extract the control parameter χ for each nucleus, the knowledge that the Pt isotopes have the O(6) symmetry was used to fix the value of η to zero for these calculations. Vanishing η values have been found in the Os nuclei as well [11] and effects of finite η values would not change the qualitative picture that emerges below. The observables $R_{4/2}$, $Q(2_1^+)$, and $B(E2;2_2^+ \rightarrow 2_1^+)$ were calculated using Hamiltonian (1) and the transition operator (2) with an constant effective charge $e=0.15$ e b. These calculated observables thus depend only on the control parameter χ as the boson number N is given. In Table I the values of χ resulting from these fits are given while Fig. 3 compares the theoretical and experimental $R_{4/2}$, $Q(2_1^+)$, and $B(E2;2_2^+ \rightarrow 2_1^+)$ as a function of χ. Note especially the change of sign in $Q(2_1^+)$ indicating the transition from prolate to oblate deformation. The experimental observables all clearly indicate the prolate-

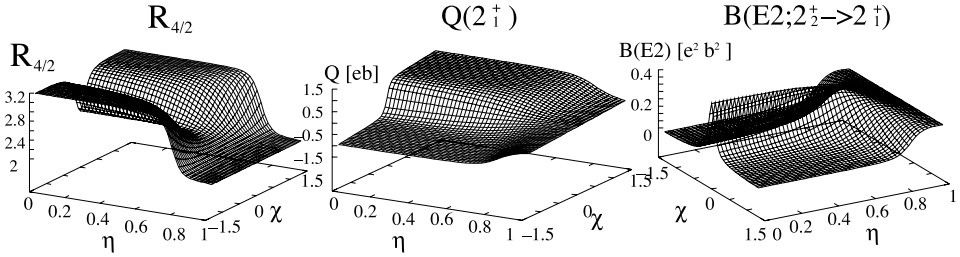

FIG. 2. $R_{4/2}$, $Q(2_1^+)$, and $B(E2;2_2^+ \rightarrow 2_1^+)$ as a function of η and χ for $N=10$. For the calculation of $Q(2_1^+)$ and $B(E2;2_2^+ \rightarrow 2_1^+)$ an effective charge of $e=0.1$ e b was used.

TABLE I. The Table lists the number of bosons N, the corresponding atomic nuclei considered here, and the deduced value for the control parameter χ (see text).

N	4	5	6	7	8	9	10	11	12	13	14
Nucleus	^{200}Hg	^{198}Hg	^{196}Pt	^{194}Pt	^{192}Os	^{190}Os	^{188}Os	^{186}W	^{184}W	^{182}W	^{180}Hf
χ	0.61	0.30	0.10	0.00	−0.15	−0.20	−0.26	−0.30	−0.39	−0.50	−0.60

oblate phase transition. The $B(E2;2_2^+\rightarrow 2_1^+)$ values and quadrupole moments are very well described in view of the very simple one-parameter Hamiltonian used. The general behavior of the quadrupole moment together with the $B(E2;2_2^+\rightarrow 2_1^+)$ values are strong indicators of a prolate-oblate phase transition. The very rapid change of the quadrupole moment and the $B(E2;2_2^+\rightarrow 2_1^+)$ values might explain why ^{196}Pt has a nonvanishing quadrupole moment although in most other respects it behaves as a good O(6) nucleus. In fact inspecting Fig. 2 one clearly notices that exactly at O(6) ($\chi=0$) there is the most significant change in these variables already for $N=10$. In view of the integer number of bosons associated with each atomic nucleus, the finite values for the quadrupole moments of the two Pt isotopes are thus also not a big surprise. The atomic nucleus ^{194}Pt seems to be the closest to the phase transition and is here fitted with $\chi=0$.

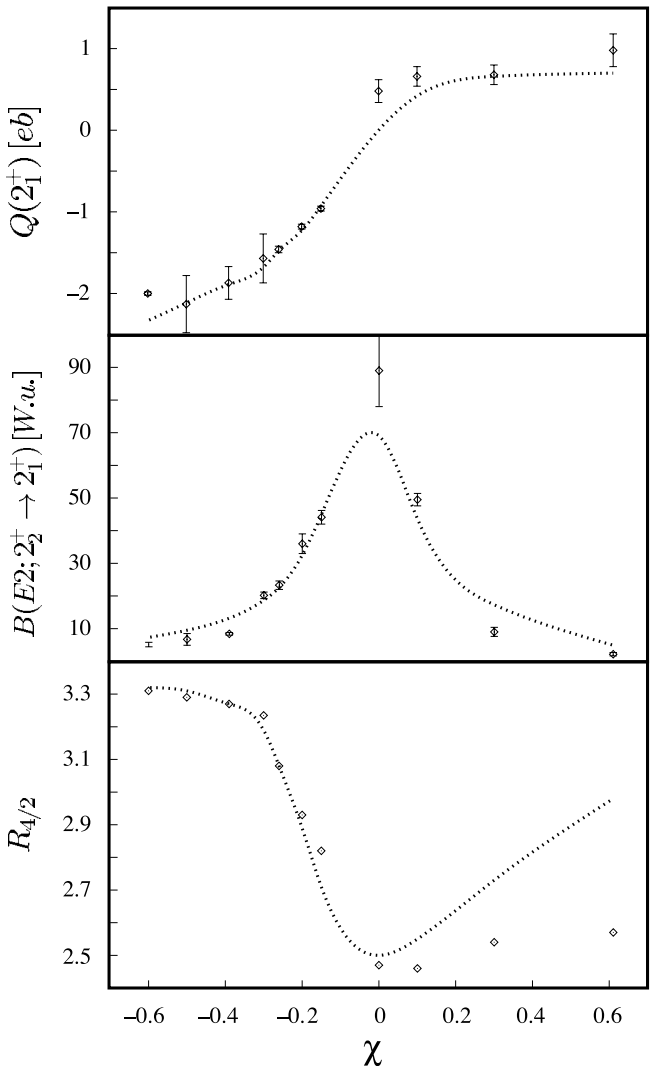

FIG. 3. Comparison between the experimental observables $R_{4/2}$, $Q(2_1^+)$, and $B(E2;2_2^+\rightarrow 2_1^+)$ for the nuclei: ^{180}Hf [18], ^{182,184,186}W [19], ^{188,190,192}Os [20], ^{194,196}Pt [21], and ^{198,200}Hg [22] and the theoretical values (dashed lines) obtained using the one-parameter Hamiltonian.

The one-parameter Hamiltonian also describes very well the $R_{4/2}$ ratio on the prolate side of the phase transition, i.e., for negative χ values. At the phase transition and on the oblate side deviations in the $R_{4/2}$ ratio are observed. In particular, the Pt isotopes have a slightly smaller $R_{4/2}$ ratio than can be achieved with the simple Hamiltonian indicating that for $N\leqslant 7$ the path is no longer on the leg but slightly inside the triangle. Surprising are the signatures for ^{198,200}Hg. While they are not very well described quantitatively by the one-parameter Hamiltonian, they qualitatively reveal unexpected features since they do not resemble a vibrational or shell model structure that might have been expected as ^{208}Pb is approached. Such structures would have $R_{4/2}$ around or below 2. Instead a slight increase in $R_{4/2}$ suggests an increase in the deformation which indicates a deviation from the U(5)-O(6) line towards $\overline{\mathrm{SU(3)}}$. The origin of the increased deformation should be related to the quenching of the pairing correlations at the oblate $Z=80$ and $N=120$ subshells [23]. Starting from ^{202}Hg the observables $R_{4/2}$ and $Q(2_1^+)$ decrease again, indicating that one is now approaching the doubly magic nucleus ^{208}Pb. Here, more knowledge on neutron-rich nuclei below $Z=82$ would be of interest.

In conclusion, we have interpreted nuclei between ^{180}Hf and ^{200}Hg as situated on or very near the SU(3)-$\overline{\mathrm{SU(3)}}$ leg of the extended Casten triangle. They exhibit a prolate-oblate phase transition in their shape which can be described at the transition by the O(6) limit of the IBM. The results obtained reinforce this new interpretation with experimental data and reveal once more how useful the general concept of phase transitions is in nature [24].

The authors want to thank R. Bijker, O. Castanos, P. Cejnar, R. F. Casten, J. Dukelski, A. Frank, P. von Brentano, S. W. Yates, and D. D. Warner for illuminating discussions on the subject of shape phase transitions, D. Balabanski for advice on the literature values for the quadrupole moments, and S. Heinze, P. Pejovic, and V. Werner for producing figures and many discussions.

[1] F. Iachello, Phys. Rev. Lett. **85**, 3580 (2000).
[2] F. Iachello, Phys. Rev. Lett. **87**, 052502 (2001).
[3] A. Bohr and B. R. Mottelson, *Nuclear Structure* (Benjamin, New York, 1975).
[4] R.F. Casten and N.V. Zamfir, Phys. Rev. Lett. **85**, 3584 (2000).
[5] R.F. Casten and N.V. Zamfir, Phys. Rev. Lett. **87**, 052503 (2001).
[6] J. Jolie, R.F. Casten, P. von Brentano, and V. Werner, Phys. Rev. Lett. **87**, 162501 (2001).
[7] F. Iachello and A. Arima, *The Interacting Boson Model* (Cambridge University Press, Cambridge, 1987).
[8] J. Jolie, P. Cejnar, R.F. Casten, S. Heinze, A. Linnemann, and V. Werner, Phys. Rev. Lett. **89**, 182502 (2002).
[9] P. Cejnar and J. Jolie, Phys. Rev. E **61**, 6237 (2000).
[10] A.E.L. Dieperink, O. Scholten, and F. Iachello, Phys. Rev. Lett. **44**, 1747 (1980).
[11] R.F. Casten and J.A. Cizewski, Nucl. Phys. **A309**, 477 (1978).
[12] D.D. Warner and R.F. Casten, Phys. Rev. C **28**, 1798 (1983).
[13] A.N. Andreyev *et al.*, Nature (London) **405**, 430 (2000).
[14] J.A. Cizewski, R.F. Casten, G.J. Smith, M.L. Stelts, W.R. Kane, H.G. Boerner, and W.F. Davidson, Phys. Rev. Lett. **40**, 167 (1978).
[15] M.P. Fewell, Phys. Lett. **167B**, 6 (1981).
[16] R.F. Casten and J.A. Cizewski, Phys. Lett. B **185**, 293 (1987).
[17] H.G. Boerner, J. Jolie, S.J. Robinson, R.F. Casten, and J.A. Cizewski, Phys. Rev. C **42**, R2271 (1990).
[18] E. Browne, Nucl. Data Sheets **71**, 81 (1996).
[19] B. Singh and R.B. Firestone, Nucl. Data Sheets **74**, 383 (1995); R.B. Firestone, *ibid.* **58**, 243 (1989); **55**, 583 (1988).
[20] B. Singh, Nucl. Data Sheets **59**, 133 (1990); **61**, 243 (1990); V.S. Shirley, *ibid.* **64**, 205 (1990).
[21] E. Browne and B. Singh, Nucl. Data Sheets **79**, 277 (1996); Zhou Chunmei, Wang Gongqing, and Tao Zhenlan, *ibid.* **83**, 145 (1998).
[22] Zhou Chunmei, Nucl. Data Sheets **74**, 259 (1995); M.R. Schmorak, *ibid.* **75**, 667 (1995).
[23] M. Vergnes, G. Berrier-Ronsin, G. Rotbard, J. Skalski, and W. Nazarewicz, Nucl. Phys. **A514**, 381 (1990).
[24] D.D. Warner, Nature (London) **420**, 614 (2002).